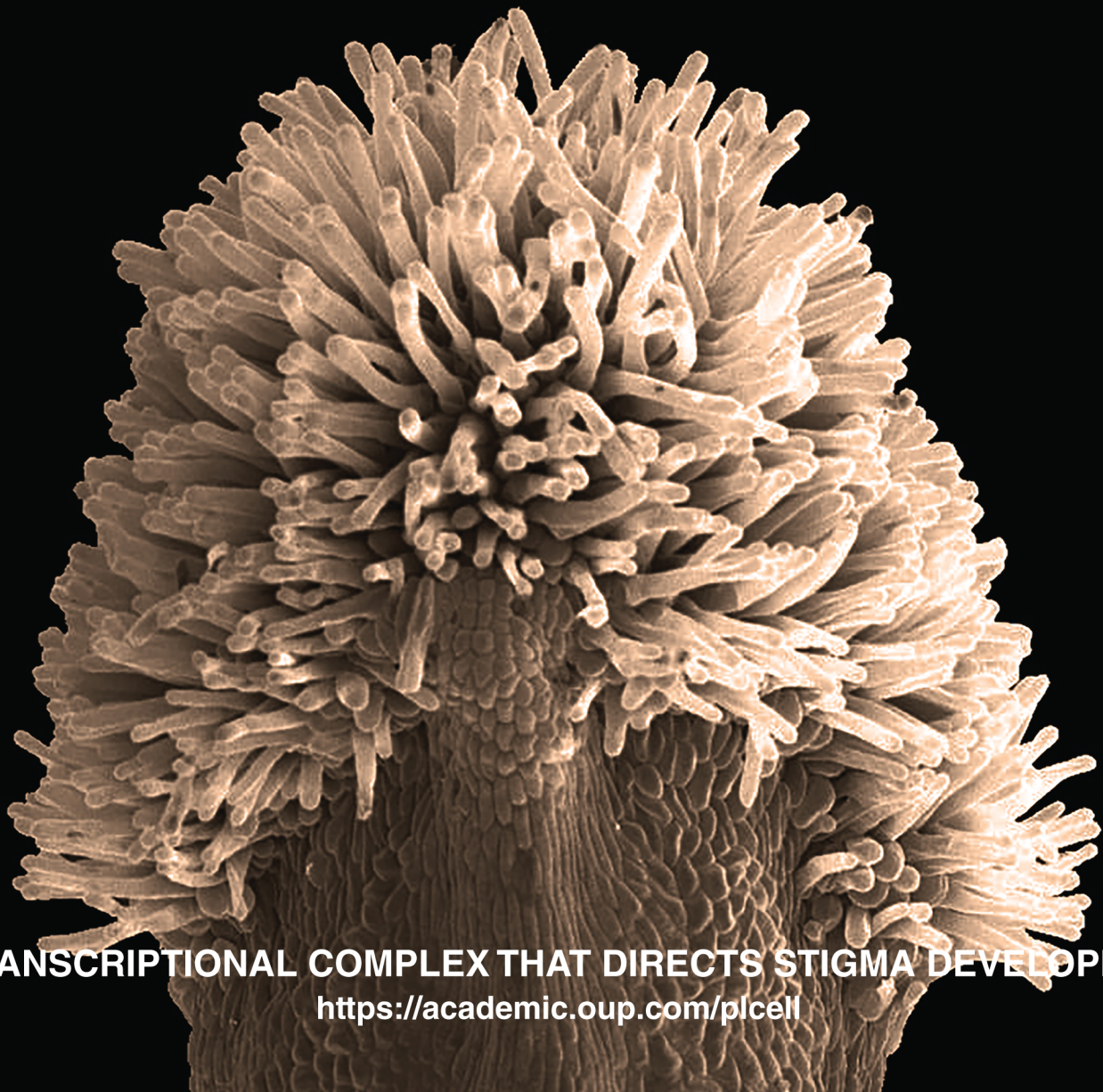


VOLUME 33

NUMBER 12

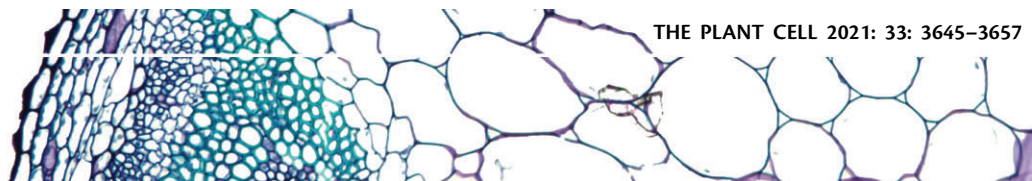
DECEMBER 2021

T H E
PLANT
C E L L



A TRANSCRIPTIONAL COMPLEX THAT DIRECTS STIGMA DEVELOPMENT

<https://academic.oup.com/plcell>



A transcriptional complex of NGATHA and bHLH transcription factors directs stigma development in *Arabidopsis*

Patricia Ballester ¹, Maria A. Martínez-Godoy,¹ Miguel Ezquerro ^{1,2}, Marisa Navarrete-Gómez,¹ Marina Trigueros ¹, Manuel Rodríguez-Concepción¹ and Cristina Ferrándiz^{1,*†}

1 Instituto de Biología Molecular y Celular de Plantas, Consejo Superior de Investigaciones Científicas, Universitat Politècnica de València, Valencia, Spain

2 Centre for Research in Agricultural Genomics (CRAG) CSIC-IRTA-UAB-UB, 08193 Barcelona, Spain

*Author for correspondence: cferrandiz@ibmcp.upv.es

†Senior author.

P.B., M.R.-C., and C.F. conceived and designed the experiments. P.B., M.A.M.-G., M.E., M.N., M.T. performed the experiments. P.B. and C.F. analyzed the data and wrote the manuscript. All authors read and approved the manuscript.

The author responsible for distribution of materials integral to the findings presented in this article in accordance with the policy described in the Instructions for Authors (<https://academic.oup.com/plcell>) is: Cristina Ferrándiz (cferrandiz@ibmcp.upv.es).

Abstract

The stigma is an angiosperm-specific tissue that is essential for pollination. In the last two decades, several transcription factors with key roles in stigma development in *Arabidopsis thaliana* have been identified. However, genetic analyses have thus far been unable to unravel the precise regulatory interactions among these transcription factors or the molecular basis for their selective roles in different spatial and temporal domains. Here, we show that the NGATHA (NGA) and HECATE (HEC) transcription factors, which are involved in different developmental processes but are both essential for stigma development, require each other to perform this function. This relationship is likely mediated by their physical interaction in the apical gynoecium. NGA/HEC transcription factors subsequently upregulate *INDEHISCENT* (*IND*) and *SPATULA* and are indispensable for the binding of *IND* to some of its targets to allow stigma differentiation. Our findings support a nonhierarchical regulatory scenario in which the combinatorial action of different transcription factors provides exquisite temporal and spatial specificity of their developmental outputs.

Introduction

Stigmas and styles are specialized tissues of the gynoecium that mediate pollination. Stigmas and styles are unique structures found only in angiosperms. The stigma, which develops at the distal region of the gynoecium, is generally formed by a single layer of elongated cells called papillae derived from the carpel marginal domain. The stigma is the receptive part of the pistil, which functions by binding to pollen grains, promoting their hydration and germination,

and providing an entry point for the pollen tubes in their path towards the ovules (Ferrándiz et al., 2010).

In *Arabidopsis thaliana*, different genes have been shown to participate in stigma development. Among these, members of two unrelated transcription factor families play essential roles in the specification of the style and stigma. The NGATHA (*NGA*) genes form a small subfamily of four highly related genes within the RAV clade of the B3-domain

IN A NUTSHELL

Background: The stigma is a specialized tissue that forms at the top of the pistil, the female organ of the flower. The stigma is essential for catching and germinating pollen grains and for ensuring that only the correct pollen species enter the pistil and fertilize the ovules. A proper stigma is key for the reproductive success of flowering plants and the production of fruits and seeds in crops. It is therefore important to understand the genetics behind stigma development. In *Arabidopsis*, several transcription factors are required for stigma formation, but most of them are also important for the development of other tissues in the pistil and even other organs outside the flower.

Question: Until now, it was not clear how these transcription factors organize the chain of command to specifically form the stigma and no other tissues at the right developmental time and spatial domain.

Findings: Using *Arabidopsis*, we performed genetic and molecular analyses to propose a model that explains how these factors work together to promote stigma differentiation. We show that there is a strict requirement for the simultaneous presence of NGATHA transcription factors and different members of the bHLH family (HECATE, INDEHISCENT, and SPATULA) to allow stigma formation. We also found that this requirement is likely mediated by the formation of a protein complex that affects the DNA binding properties of these factors to their targets. The composition and the dynamic incorporation of the different factors to the complex may explain the specificity of its developmental outcome: we propose that these multifunctional transcription factors achieve specificity in their common role in stigma development by overlapping in time and space.

Next steps: We want to know if similar complexes direct stigma formation in other species, and if this evolutionary novelty might be linked to tinkering with ancestral factors that gained the ability to combine and produce this new tissue, which is characteristic of (and specific to) flowering plants. Also, we want to know if different combinations of these and additional transcription factors could direct the formation of other pistil tissues, such the style or ovary.

transcription factor family. NGA transcription factors act redundantly to direct style and stigma development: while single *nga* mutants only show weak defects in style formation, *nga* triple and quadruple mutants completely lack all the apical tissues of the gynoecium but have relatively unaffected ovaries (Alvarez et al., 2009; Trigueros et al., 2009). Members of the SHORT INTERNODES/STYLISH (SHI/STY) family of zinc-finger transcription factors also act redundantly in these same processes, as *shi/sty* higher-order mutant combinations have very similar phenotypes to those of *nga* mutant combinations (Kuusk et al., 2006). Importantly, the roles of NGA and SHI/STY transcription factors in apical gynoecium development are widely conserved, indicating their prominent importance in gynoecium morphogenesis (Fourquin and Ferrandiz, 2014; Gomariz-Fernandez et al., 2017).

In addition to these genes families, other transcription factors of the basic helix–loop–helix (bHLH) family are also required for apical pistil development. Mutants in the SPATULA (*SPT*) gene have a reduced stigma, partially unfused style, and defects in the development of transmitting tissues (Alvarez and Smyth, 1999; Heisler et al., 2001). Likewise, HECATE (*HEC*) genes are required for transmitting tract and stigma differentiation in a redundant manner. Triple *hec1 hec2 hec3* mutants completely lack stigmatic papillae and the internal transmitting tissues of the style and the septum, although the outer morphology of the style shows only mild defects. INDEHISCENT (*IND*) is the closest paralog to *HEC* genes in *Arabidopsis*. *IND* function has mainly been associated with the development of the dehiscence zone of the fruit, but *ind* mutants also show subtle

defects in stigmatic papillae elongation that are dramatically enhanced when combined with mutations in *SPT* and thus, the apical tissues of *ind spt* pistils closely resemble those of *hec* triple mutants (Liljegen et al., 2004; Girin et al., 2011).

In addition to these common functions in apical gynoecium development, *HEC*, *SPT*, *NGA*, and *SHI/STY* genes also have more general roles in lateral organ development or meristem function, where they control the balance between cell proliferation and differentiation, partly via direct regulation of auxin and cytokinin signaling (Eklund et al., 2010; Sidaway-Lee et al., 2010; Josse et al., 2011; Reymond et al., 2012; Baylis et al., 2013; Schuster et al., 2014; Gaillochet et al., 2017; Reyes-Olalde et al., 2017). These functional similarities indicate that all these factors are part of common or convergent regulatory pathways directing morphogenesis. Various studies have revealed some of the regulatory interactions among these factors. *SPT* has been shown to physically interact with *IND* to regulate common targets required for polar auxin transport, such as the AGC kinase genes *PINOID* (*PID*) and *WAG2* (Girin et al., 2011). *SPT* is able to heterodimerize with *HEC* transcription factors. These interactions likely mediate their common roles in regulating auxin and cytokinin signaling, both at the shoot apical meristem (SAM) and during gynoecium development (Gremski et al., 2007; Gaillochet et al., 2017; Reyes-Olalde et al., 2017). *NGA1* and *NGA2*, on the other hand, are direct targets of *HEC1* that participate in stem cell regulation at the SAM in both *HEC*-dependent and -independent pathways (Gaillochet et al., 2017). Altogether, these findings point to an intricate functional relationship among all these factors. However, the precise nature of their genetic interactions is not fully solved.

In this study, we specifically focused on characterizing the regulatory interactions of NGA and bHLH transcription factors in the context of gynoecium development. Our results unravel a regulatory network where NGA and HEC transcription factors interact cooperatively to upregulate *IND* and *SPT*. Further downstream, they all appear to form a multimeric complex required for stigma development and correct auxin distribution.

Results

hec mutations suppress the phenotype of NGA-overexpressing plants

Constitutive expression of either *HEC* or *NGA* transcription factor genes causes developmental defects. In addition, the defects in stigma and tract formation of Arabidopsis *hec* mutants can be considered a subset of those found in *nga* quadruple mutants, which completely lack apical tissues (Gremski et al., 2007; Alvarez et al., 2009; Trigueros et al., 2009), suggesting that *HEC* genes might be acting downstream of *NGA* to direct gynoecium development. To test this hypothesis, we introduced the *NGA3* transgene driven by the constitutive 35S promoter (p35S:NGA3) into the *hec1 hec3* background. As previously described, *hec1 hec3* mutants have no conspicuous defects in plant architecture but show mild defects in stigma and transmitting tract development that cause reduced fertility and smaller fruit size (Figure 1, A and H). In contrast, p35S:NGA3 plants in

the wild-type background develop pistils and fruits with long gynophores, reduced ovaries, and enlarged misshapen repla (central ridges between valves; Figure 1, A–C, F, G, J, K, N, O); these lines also show vegetative phenotypic defects, such as short stature, narrow leaves, and reduced apical dominance (Trigueros et al., 2009; Supplemental Figure S1). Surprisingly, the p35S:NGA3 *hec1 hec3* plants were almost indistinguishable from the *hec1 hec3* mutants. The elongated gynophores, wide replum, and small valves typical of p35S:NGA3 fruits were restored to those found in *hec1 hec3* fruits (Figure 1, A, D, E, H, I, L, M, P, and Q). Moreover, in p35S:NGA3 *hec1 hec3* plants, overall plant morphology defects typical of p35S:NGA3 lines were also suppressed, and the leaves were no longer narrow and epinastic as in p35S:NGA3 but had a wild-type morphology, as seen in *hec1 hec3* mutants (Supplemental Figure S1). Thus, the *hec1 hec3* mutations largely suppressed the p35S:NGA3 phenotype. In the segregating population from this cross, p35S:NGA3 *hec3* plants were also identified; these plants showed a partial but significant suppression of the *NGA3* overexpression phenotype: gynophores were slightly longer than in the wild-type or *hec3*, the replum width was restored, and the fruits were similar in size to *hec3* fruits but had a bumpier appearance (Supplemental Figure S1). This partial suppression of the p35S:NGA3 phenotype was not observed in p35S:NGA3 *hec1* plants, suggesting that *HEC3* plays a major role in mediating *NGA3* activity.

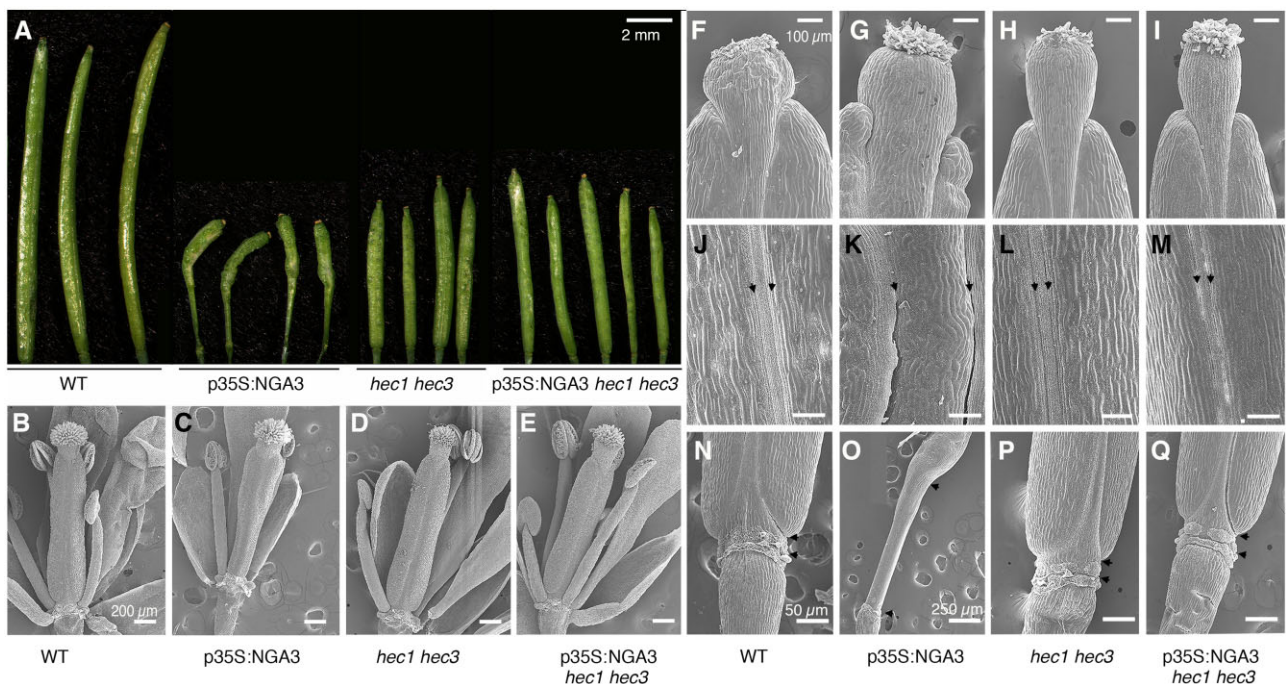


Figure 1 The phenotype of *NGA3*-overexpressing plants is suppressed by the *hec1 hec3* mutations. A, Fully elongated fruits of the wild-type (Col), p35S:NGA3, *hec1 hec3* double mutants, and p35S:NGA3 *hec1 hec3* lines. B–E, Scanning electron micrographs of pistils at anthesis in the wild-type (B), p35S:NGA3 (C), *hec1 hec3* (D), and p35S:NGA3 *hec1 hec3* (E). Bars represent 200 μ m. F–Q, Scanning electron micrographs of different regions of fully elongated fruits: F–I, stigma and style, bars represent 100 μ m; J–M, central section of the ovary, bars represent 100 μ m, black arrows in J–M mark the position of the valve margins and thus the replum width; N–Q, gynophore and basal ovary, bars represent 50 μ m in N, P, Q, 250 μ m in O; black arrows mark the two ends of the gynophore. F, J, N, wild-type; G, K, O, p35S:NGA3; H, L, P, *hec1 hec3*; I, M, Q, p35S:NGA3 *hec1 hec3*.

These results could be explained if NGA transcription factors upregulated *HEC* genes and therefore, the ectopic and elevated expression of *HEC* genes in the p35S:NGA3 background mediated the *NGA* overexpression phenotype. To test this idea, we introduced pHEC:GUS reporters into both loss- and gain-of-function *NGA* lines. Surprisingly, the spatial expression patterns of the three *HEC* reporters in both backgrounds were largely unaffected in both vegetative and reproductive tissues (Figure 2, A–O), except in the apical domain of the mature gynoecia of *nga* multiple mutants, where it was reduced, likely due to the absence of stigma and style differentiation (Figure 2, C, F, and I). However, in earlier stages of flower development, *HEC* expression in the apical domain of *nga* gynoecium primordia was clearly observed (Figure 2, M–S), suggesting that the activation of *HEC* genes in these domains could occur independently of *NGA* function. While the spatial expression patterns of the reporter lines were similar in the three backgrounds, the activity of *HEC* reporters was lower in *nga* flowers and higher in p35S:NGA3 flowers, as further confirmed by quantitative reverse transcription polymerase chain reaction (qRT-PCR) analyses of the expression of all three *HEC* genes in these backgrounds (Figure 2T). Considering that the phenotype caused by *NGA3* overexpression in flowers, leaves, and

overall plant morphology was largely suppressed in the *hec1 hec3* background, it appeared unlikely that only changes in the expression levels of *HEC* genes could be responsible for the strong developmental defects observed in p35S:NGA3 plants.

NGA and HEC transcription factors require each other for function

These results led us to propose an alternative hypothesis in which *NGA* transcription factors would require *HEC* activity to perform their functions as a protein complex. We detected a clear interaction of *HEC1* and *HEC3* proteins with *NGA1* and *NGA3* transcription factors by bimolecular fluorescent complementation (BiFC) experiments in *Nicotiana benthamiana* leaves (Figure 3A). Thus, if *NGA/HEC* protein complex formation was required for their function, the overexpression of *HEC* in a *nga* mutant background should have little effect on development. We therefore generated transgenic plants by introducing a p35S:*HEC1* or a p35S:*HEC3* construct in *nga2 nga3 nga4* mutants, which have similar phenotypes to the quadruple *nga* mutant but are still able to form a small number of seeds. When transformed into the wild-type background, p35S:*HEC1* and p35S:*HEC3* caused similar alterations in development, also

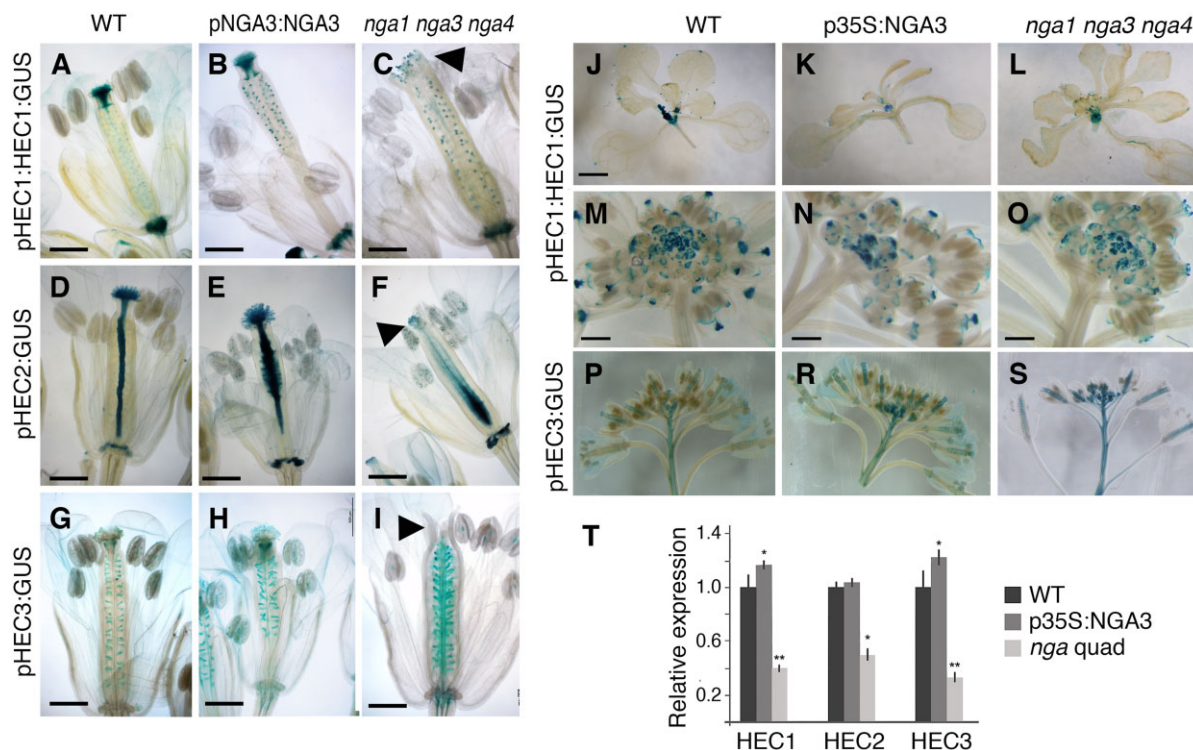


Figure 2 *HEC* spatial expression is not significantly affected by the loss or gain of *NGA* function. A–I, *HEC* reporter activity in flowers at anthesis in the wild-type (A, D, and G), p35S:NGA3 (B, E, and H), and *nga1 nga3 nga4* triple mutants (C, F, I). pHEC1:HEC1:GUS is shown in (A–C), pHEC2:GUS in (D–F), and pHEC3:GUS in (G–I). Arrows in C, F, and I indicate apical domain of the pistil, where *HEC* reporter activity is highly reduced but detectable. Bars represent 200 μ m. (J–O) pHEC1:HEC1:GUS reporter activity in 10-day-old seedlings (J–L) and in inflorescences (M–O) of the wild-type (J and M), p35S:NGA3 (K and N), and *nga1 nga3 nga4* (L and O). Bars represent 1 mM. P–S, pHEC3:GUS reporter activity in inflorescences of the wild-type (P), p35S:NGA3 (R), and *nga1 nga3 nga4* triple mutant (S). Bars represent 1-mM (T) qPCR analysis of *HEC* gene expression in inflorescences of the wild-type, p35S:NGA3, and *nga* quadruple mutants. Expression relative to wild-type levels is represented, with standard deviation for three biological replicates. * $P < 0.05$, ** $P < 0.01$.

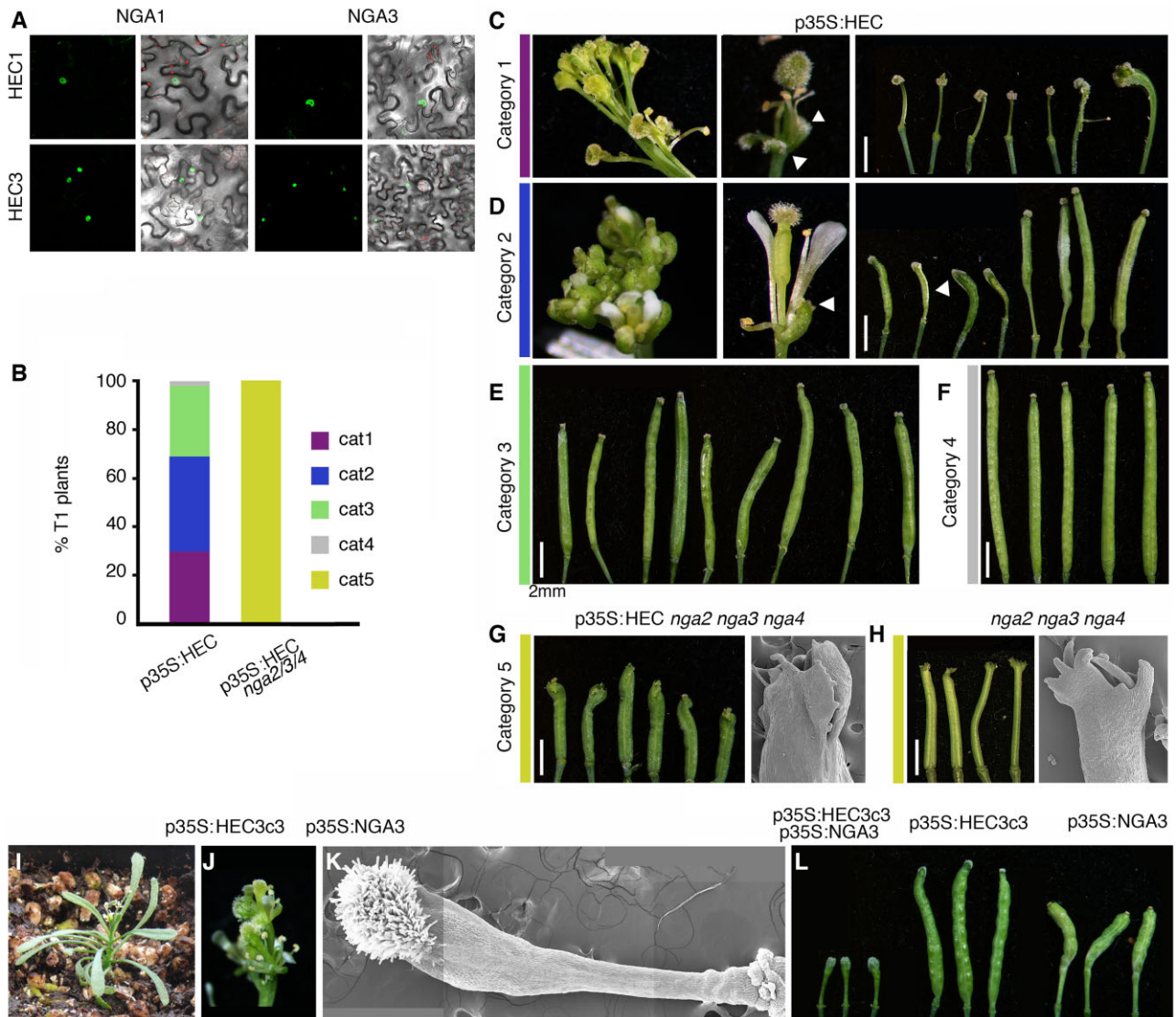


Figure 3 HEC transcription factors require NGA to promote stigma development and to alter apical-basal development of the pistil. **A**, BiFC experiments showing that HEC1 and HEC3 are able to interact physically with NGA1 and NGA3. **B–H**, Effect of HEC1 or HEC3 overexpression on gynoecium development. **B**, Proportion of phenotypic categories of T1 lines transformed with p35S:HEC constructs according to the categories shown in (C–G). **C–F**, Representative fruit and inflorescence morphologies of T1 wild-type plants transformed with p35S:HEC1 or p35S:HEC3 constructs belonging to different phenotypic categories: category 1, strong (C); category 2, intermediate (D); category 3, weak (E); category 4, similar to the wild-type (F). **G** Representative fruit morphology of *nga2 nga3 nga4* mutants transformed with p35S:HEC1 or p35S:HEC3 (left, category 5), and scanning electron micrograph of the apical domain of the fruit (right). **H**, Fruit morphology of *nga2 nga3 nga4* mutants (left), and scanning electron micrograph of the apical domain of the fruit (right). Fruits in category 5 of transformed plants in (G) are identical to those in (H). **I–L**, Phenotypic effect of simultaneous overexpression of HEC3 and NGA3 generated by crossing a p35S:HEC3 line with weak phenotypic defects (category 3) and the p35S:NGA3 line. All photographs show F1 descendants from this cross. **I**, Morphology of the whole plant resulting from this cross. The rosette forms narrow leaves and is approximately 2-cm wide. The inflorescence is short and fasciated. **J**, Close-up of the inflorescence in (I), showing a compact group of highly abnormal flowers that lack most floral organs except pistils and are sterile but develop parthenocarpically to a certain degree. **K**, Scanning electron micrograph of a fruit from the line shown in (I). The fruit is very reduced in size, consisting of a long gynophore, a highly modified and reduced ovary-like structure where the cell morphologies of valves, valve margins, replum, and style are not clearly defined, and extensive stigmatic tissue in the apical part. **L**, Representative fruits from the line shown in (I) and the parental lines used for crossing. White arrows in C and D mark ectopic stigmatic tissue developing at the tip of sepaloid organs in whorl 1 (B and C, central parts) or the replum of fruits (C, right).

equivalent to those already described in other studies (Gremski et al., 2007), which ranged in severity in individual T1 plants ($n = 54$ for p35S:HEC1 and $n = 67$ for p35S:HEC3). The most affected lines (~30% of the combined p35S:HEC lines, category 1 in Figure 3, B and C) developed very

compact inflorescences, often fasciated, where carpeloid structures developed frequently in place of flowers and extensive stigma development was present in the outer whorls of the flower (Figure 3, B and C). These carpel-like organs had very reduced or absent valves and enlarged stigmatic

domains, resembling those of *pid* or *pin-formed* (*pin*) mutants, and were fully sterile. About 38% of the plants (category 2; Figure 3, B and D) showed malformed flowers where gynoecia had weakly elongated gynophores, a variable number of valves, and ectopic stigma formation along the repla and occasionally at the tip of the sepals. Around 30% of the lines were classified in category 3 (Figure 3, B and E), which comprised plants with weak defects in carpel and fruit development, such as elongated and malformed styles, irregular valve surfaces, or smaller fruit size. Finally, 2% of the T1 plants were indistinguishable from the wild-type (category 4; Figure 3, B and F). Strikingly, when p35S:HEC1 or p35S:HEC3 was transformed in the *nga2 nga3 nga4* background, all transgenic T1 lines ($n = 39$ for p35S:HEC1 and $n = 26$ for p35S:HEC3) showed the typical *nga* multiple mutant phenotype and none of the phenotypes in categories 1, 2, or 3 previously described for the overexpression of *HEC* in a wild-type background (category 5; Figure 3, B, G, and H). These results indicate that the phenotype caused by *HEC* overexpression was largely dependent on the presence of *NGA* transcription factors.

Moreover, when the p35S:HEC1 or the p35S:HEC3 constructs were transformed into the p35S:NGA3 background, we could not identify primary transformants, suggesting that the simultaneous overexpression of *NGA* and *HEC* might cause seedling lethality. To overcome this possible effect, a p35S:HEC3 line classified in phenotypic category 3 (weak defects in fruit development, p35S:HEC3c3) was crossed with the p35S:NGA3 line and a few seeds were obtained. The progeny of such cross showed a strong phenotypic enhancement with respect to the parental lines (Figure 3, I–L). The adult plants were extremely reduced in size, with small narrow leaves and reduced inflorescences that produced a limited number of flowers (Figure 3I). Sepals, petals, and stamens, which appeared in variable numbers, were misshapen and frequently developed ectopic stigmatic tissue at their distal domains (Figure 3J). The gynoecia of these flowers were also very small, with elongated gynophores, no clear demarcation of the valves, replum, or style regions, and extensive development of stigmatic tissue, indicating that the ectopic co-expression of both transcription factors produced novel synergistic alterations in development (Figure 3, K and L). Altogether, these results suggest that *NGA* and *HEC* transcription factors work cooperatively and require each other to elicit developmental responses, including stigma formation.

To further study the regulatory interactions between *NGA* and *HEC* transcription factors, we also tested how the loss or gain of *HEC* function affected the spatial activity of the pNGA3:GUS reporter. pNGA3:GUS expression was very similar in the wild-type, *hec1 hec3*, or p35S:HEC3 backgrounds, which is similar to what we observed for pHEC:GUS reporters in the *nga* or p35S:NGA3 backgrounds (Figure 4, A–C). These results further indicate that the expression of *HEC* and *NGA* genes is initially established independently of their mutual regulation and that their synergistic effects on development could be mediated by protein interaction.

NGA and HEC jointly regulate SPT and IND in the developing gynoecium and fruit

Different studies have uncovered the functional interaction of *HEC*, *SPT*, and *IND*. The apical domain of *hec1 hec2 hec3* pistils closely resembles those of the double *spt ind* mutants. In addition, *SPT* protein is able to interact with *HEC* proteins and with *IND*, the closest paralog to *HEC3*. Moreover, plants overexpressing *IND* resemble those overexpressing *HEC* genes (Gremski et al., 2007; Girin et al., 2011; Schuster et al., 2015). Interestingly, it has been shown that *IND* activates *SPT* expression and that, once *SPT* is present, they both cooperatively regulate the expression of genes involved in auxin transport, such as *PID* and *WAG2*. This cooperative action appears to be mediated by the physical interaction of *SPT* and *IND*, and, accordingly, the phenotype caused by *IND* overexpression is largely dependent on the presence of *SPT* (Girin et al., 2011).

Since *NGA* and *HEC* transcription factors appeared to work cooperatively, also likely as a protein complex, we wondered whether this *HEC*–*NGA* complex could act in a similar manner to *IND*–*SPT*. Moreover, based on the related phenotypes of *hec1 hec2 hec3* and *ind spt* mutants or the p35S:HEC and the p35S:IND lines, we further speculated that *IND* and/or *SPT* could be also targets of *HEC*–*NGA*.

To test these hypotheses, we first investigated the genetic relationship of *NGA* with *IND* and *SPT*. *IND* expression was expanded to the valves and stronger in the style domain of p35S:NGA3 stage 11 gynoecia (Figure 5, A and B), but not when *hec1 hec3* mutations were also present (Figure 5C); conversely, the expression of *IND* in the distal part of the developing gynoecia was absent when *NGA* function was reduced by the presence of an amiRNA-*NGA* transgene, while the expression in the valve margin was unaffected (Figure 5D). This suggests that *NGA* acts upstream of *IND*, but that this regulation requires additional factors, since *NGA3* overexpression did not result in constitutive *IND* upregulation and was mainly limited to its expansion to the valves. Moreover, both the p35S:NGA3 *ind* and p35S:NGA3 *spt* combinations resulted in a partial suppression of the *NGA3* overexpression phenotype in gynoecia and fruits

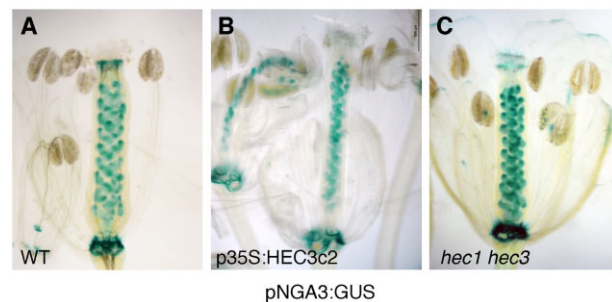


Figure 4 *NGA3* spatial expression is not significantly affected by the loss or gain of *HEC* function. A–C, Activity of a pNGA3:GUS reporter in pistils during anthesis from the wild-type (A), p35S:HEC3 belonging to category 2 as defined in Figure 3 (intermediate), and *hec1 hec3* double mutant.

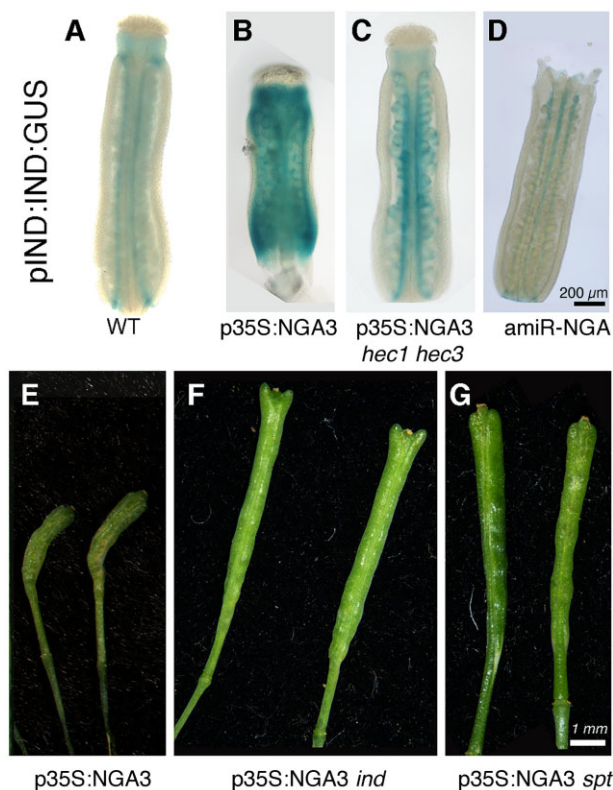


Figure 5 *IND* is upregulated by NGA transcription factors and is partially required for the NGA3 overexpression phenotype in fruits. A–D, Activity of an pIND:IND:GUS reporter in pistils during anthesis in the wild-type (A), p35S:NGA3 (B), p35S:NGA3 *hec1 hec3* (C), and a knock down line where the expression of all NGA genes is reduced by overexpression of the amiR-NGA described in Trigueros et al. (2009). Constitutive expression of NGA3 in a wild-type background causes a conspicuous increase in *IND* expression in the stigma/style boundary and its expansion to the valves in the ovary. This increased and wide expression is no longer observed in the absence of HEC1/HEC3. In the amiR-NGA line, *IND* is expressed normally in valve margins, but no longer in the apical domain of the pistil. E–F, Representative fruit morphology caused by NGA3 overexpression in the wild-type (E), *ind* (F), and *spt* (G) backgrounds. The fruit phenotype caused by NGA3 overexpression is partially suppressed by *ind* and *spt* mutations.

(Figure 5, E–G). Altogether, these results suggest that the putative NGA/HEC complex acts upstream of *IND* and *SPT*.

The absence of stigma in *ind spt* double mutants and the extensive ectopic stigmatic tissue differentiation caused by *IND* overexpression suggest that stigma development depends ultimately on the direct or indirect activation of *IND* and *SPT* by the NGA/HEC complex. If this were true, *nga* or *hec* mutants overexpressing *IND* should still be able to produce ectopic stigmatic tissue. We obtained the p35S:IND:GR line, whose phenotype is only observed after Dexamethasone (Dex) treatment, introduced it into *nga1 nga3 nga4* and *hec1 hec3* plants, and assessed the effect of *IND* induction via the application of Dex to these plants. Overexpression of *IND* in the wild-type background produced compact inflorescences with severely affected flowers that showed reduced floral organs, abnormal in shape, and

pistils capped by extensive stigmatic tissue that often also developed ectopically in the distal parts of other floral organs (Figure 6, A and B). Induction of *IND* in the *nga* mutant background also produced compact inflorescences with short floral organs, but the pistils had the typical morphology of *nga* mutants, and the development of stigmatic tissue was completely prevented (Figure 6, C and D). The overexpression of *IND* the *hec1 hec3* background and the overexpression of *HEC* in *ind* mutants caused related phenotypic alterations similar to those observed when either *IND* or *HEC* were overexpressed in the wild-type background (Figure 6, E–H). These results indicate that *HEC* and *IND* proteins have similar activities, as could be expected by their sequence homology, and suggesting that they could function redundantly. Interestingly, *HEC* overexpression phenotypes were also reduced in the *spt* background, as previously described for p35S:IND *spt* lines, supporting the functional similarity of *IND* and *HEC* proteins (Figure 6). Finally, the simultaneous overexpression of *IND* and *NGA3* resulted in a synergistic effect, where inflorescences terminated in pin-like structures and the flowers were replaced by masses of stigmatic tissue with no visible floral organ differentiation (Figure 6I).

These results argued against a simple regulatory hierarchy where NGA/HEC would upregulate *IND* and then, upon *SPT* activation, the SPT/IND heterodimer would drive stigma differentiation. The requirement for NGA and *SPT* transcription factors by *IND*/HEC to carry out these functions suggests that NGA, *IND*/HEC, and *SPT* should be present simultaneously. *IND*–*SPT* and *HEC*–*SPT* protein interactions have already been reported (Gremski et al., 2007; Girin et al., 2011). Using BiFC experiments, we found that *HEC* and NGA transcription factors were also able to interact with *IND* and with *SPT* (Figure 7A). Co-immunoprecipitation (Co-IP) experiments using tagged proteins produced in *N. benthamiana* leaves confirmed the proposed interaction of NGA3 with *IND* and *SPT* and also with *HEC1* and *HEC3* proteins (Figure 7B).

Taking all this evidence together, we speculated that *IND*/HEC, *SPT*, and NGA could form a higher-order complex that would act on common targets. Good candidates for common downstream genes were *PID* and *WAG2*, which are direct targets of *IND* and *SPT* whose expression is also regulated by NGA in the distal developing gynoecium (Girin et al., 2011; Martinez-Fernandez et al., 2014). *IND* activates *SPT* expression during pistil development. Moreover, *IND* was shown to bind to an E-box variant in the *PID* promoter, and the regulation of *PID* and *WAG2* expression by *IND* was dependent on the presence of *SPT* (Girin et al., 2011). We used a similar approach to test whether *IND* also requires NGA transcription factors to regulate the *PID*, *WAG2*, and *SPT* promoters using the p35S:IND:GR and p35S:IND:GR *nga1 nga3 nga4* lines to perform a chromatin immunoprecipitation (ChIP) experiment, followed by qRT-PCR analyses of the precipitated DNA.

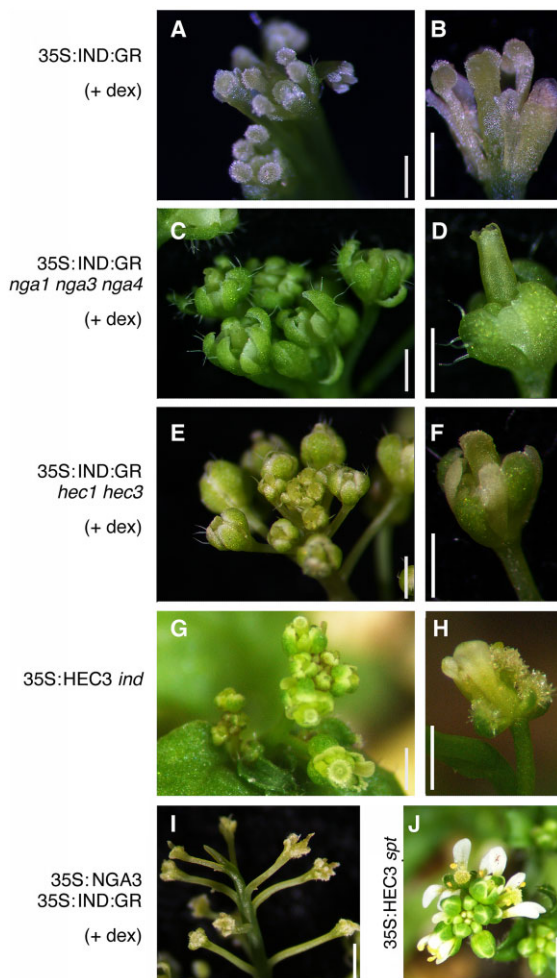


Figure 6 IND requires NGA activity to direct stigma formation. A and B, Phenotypic defects caused by the induction of constitutive IND activity in wild-type inflorescences (A) and flowers (B). Inflorescences are compact and fasciated, with strong defects in floral formation. Extensive stigma development is observed in the tips of most floral organs. Petal development is largely abolished. C, D, Phenotypic defects caused by the induction of constitutive IND activity in the *nga1 nga3 nga4* background. Inflorescences (C) are abnormal but less compact than in (A). In flowers (D), sepals are short and petal and stamen development is strongly affected, but stigma formation is never observed in the apical domain of the pistil, where ovary development appears unaffected, nor in other floral organs. E and F, Phenotypic defects caused by the induction of constitutive IND activity in the *hec1 hec3* background. The severity of phenotypic alterations in inflorescence (E) and flower (F) development is slightly reduced compared with (A and B), but extensive stigma formation and altered apical-basal development in the pistil are similar to the changes caused by IND induction in the wild-type (B). G and H, Phenotypic defects caused by constitutive HEC3 activity in the *ind* mutant background. The phenotypic defects in inflorescences (G) and flowers (H) resemble those shown in (E and F), and ectopic stigma formation is clearly observed. I, Phenotypic defects caused by the induction of constitutive IND activity in the *p35S:NGA3* background. Flowers are replaced by masses of stigmatic tissue and terminate in a pin-like structure. J, Phenotypic defects caused by constitutive HEC3 activity in the *spt* mutant background. The lack of SPT activity largely suppresses the altered inflorescence and flower development observed in the other lines. Scale bars in all parts represent 1 mm.

We found significant enrichment of fragments of the *SPT*, *PID*, and *WAG2* promoters in Dex-treated *p35S:IND:GR* plants compared with mock-treated plants, while no enrichment for any of the assayed fragments could be detected in Dex-treated *p35S:IND:GR nga1 nga3 nga4* plants compared with mock-treated plants (Figure 7C). We also tested the transcriptional responses of *SPT*, *PID*, and *WAG2* to IND induction in the same backgrounds, *p35S:IND:GR* and *p35S:IND:GR nga1 nga3 nga4*. Confirming previously reported studies, the induction of IND activity in the wild-type background caused *SPT* and *WAG2* upregulation and *PID* downregulation (Figure 7D). However, when IND activity was induced in the *nga* mutant background, only *SPT* expression was significantly activated, although at much lower levels than upon IND induction in the wild-type background (Figure 7D). These results suggest that NGA transcription factors are required by IND to regulate these downstream genes, likely by facilitating IND binding to at least some of its target promoters, as has been proposed for *SPT* (Girin et al., 2011). These findings support the hypothesis that an IND–SPT–NGA functional complex directs apical gynoecium morphogenesis and stigma development.

Discussion

Several transcription factors and components of hormone signaling pathways have been shown to play crucial roles in stigma development. Most of these transcription factors also participate in other developmental processes, as could be expected since carpels, like all floral organs, share a basic bauplan (body plan) with leaves (Kuusk et al., 2006; Alvarez et al., 2009, 2016; Trigueros et al., 2009; Ichihashi et al., 2010; Baylis et al., 2013; Ballester et al., 2015). However, genetic analyses have thus far been unable to precisely dissect the gene regulatory networks directing stigma development, and how the basic set of key genes interacts with each other to provide enough specificity to their function in gynoecium development, as opposed to their roles in leaf, flower, or meristem development. In this work, we show how the formation of protein complexes among some of transcription factors with major roles in stigma formation appears to be crucial for their function in this domain. Our results indicate that the formation of these complexes, or at least their simultaneous presence, affects the transcriptional output of these transcription factors. This could explain how they provide spatial and temporal specificity to direct stigma development thanks to their partially overlapping expression domains.

NGA transcription factors are essential for apical gynoecium formation, as inferred from the phenotypes of multiple mutants that lack stigmas and styles but show largely unaffected ovaries (Alvarez et al., 2009; Trigueros et al., 2009). It was thus conceivable to place them upstream of HEC transcription factors, which are only essential for stigma formation. However, previous reports showed that *NGA1* and *NGA2* are directly regulated by *HEC1*, suggesting that their regulatory interactions were not simple (Gaillochet et al.,

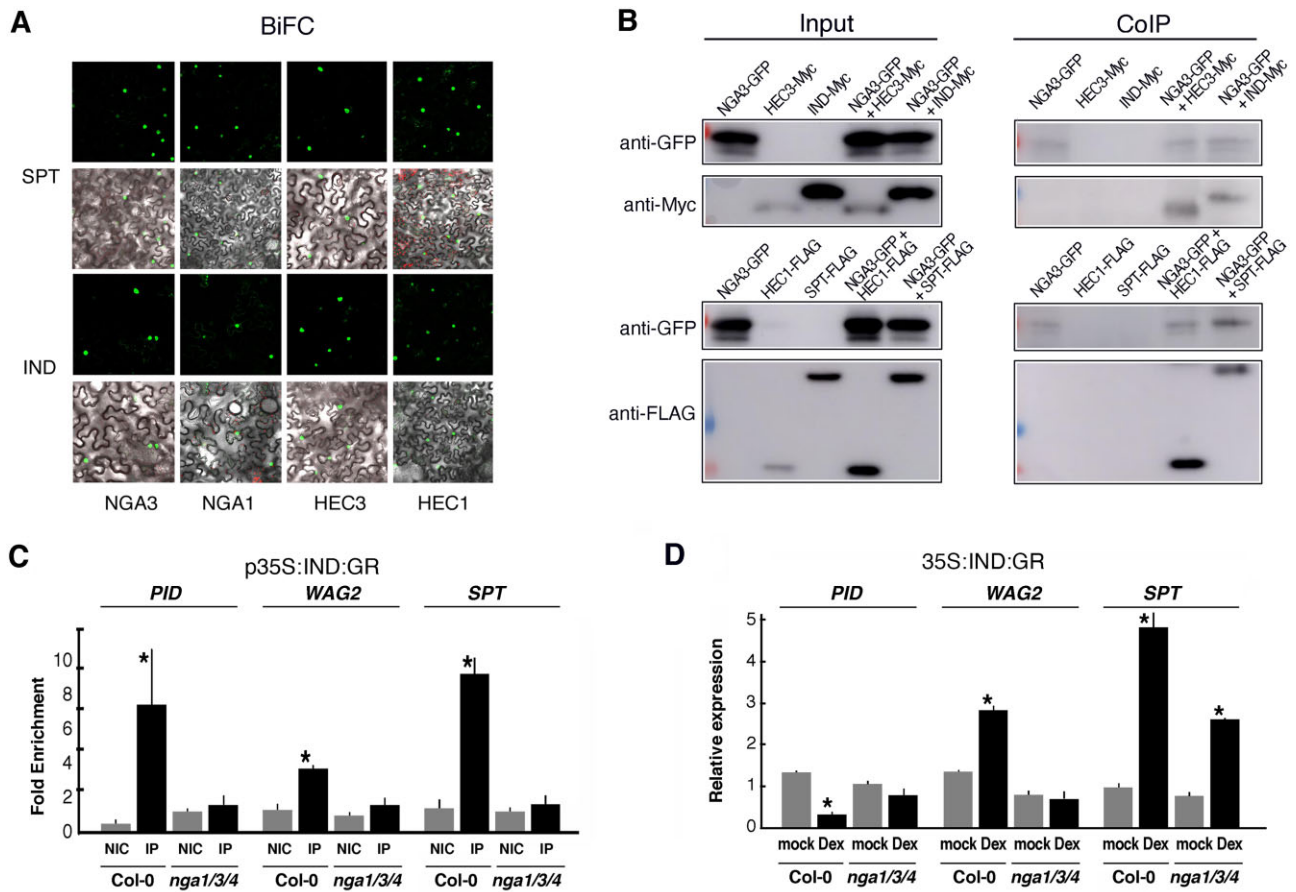


Figure 7 A and B, HEC, SPT, and IND are able to physically interact with NGA transcription factors. A, BiFC experiments showing that SPT and IND can physically interact with NGA1, NGA3, HEC1, and HEC3. Negative controls are provided in Supplemental Figure S2. B, Co-IP of NGA3-GFP- and HEC3-Myc, IND-Myc, HEC1-FLAG, and SPT-FLAG-tagged proteins in *Agrobacterium*-infiltrated *N. benthamiana* leaves. Extracts were immunoprecipitated with anti-GFP antibody and detected using anti-GFP and anti-MYC or anti-FLAG antibodies. The experiment was repeated three times with similar results. C and D, IND requires NGA to bind to its target promoters and to regulate gene expression. C, ChIP experiment against *PID*, *WAG2*, and *SPT* promoter regions previously reported to have IND binding sites, using the inducible p35S:IND:GR line in the wild-type and *nga1 nga3 nga4* backgrounds, after Dex treatment. NIC, nonimmunoprecipitated control; IP, immunoprecipitated chromatin. Error bars represent standard deviation of three biological replicates. **P* < 0.05. D, *PID*, *WAG2*, and *SPT* expression in p35S:IND:GR lines in the wild-type and *nga1 nga3 nga4* backgrounds measured by qRT-PCR. The response to IND induction by Dex was compared with that of mock-treated plants. Error bars represent standard deviation of three biological replicates. **P* < 0.05.

2018). In this study, we used genetic analyses to elucidate the nature of the functional interaction of NGA and HEC transcription factors in the context of the gynoecium. Our work shows that the effects on plant morphology caused by constitutive *NGA3* expression are dependent on the presence of HEC functional proteins (more importantly HEC3) and that, conversely, the gynoecium phenotypes caused by *HEC* overexpression are fully suppressed by *nga* mutations.

Based on these findings, together with (1) the low impact of *NGA* loss or gain-of-function on *HEC* spatial regulation and vice versa, (2) the strong synergistic effects of simultaneous overexpression of HEC and NGA transcription factors, and (3) the physical interaction observed between both types of proteins, we propose that an obligate heterodimerization has to take place to enable some HEC and NGA functions and, in particular, to activate the pathway leading to stigma formation. This heterodimer, which might be part

of a higher-order complex of yet unknown composition and stoichiometry, would participate (directly or indirectly) in the upregulation of *IND*, and subsequently of *SPT*, in the apical gynoecium. Then, once *IND* and *SPT* were activated, they would still require the presence of NGA transcription factors for *IND* binding to some of its targets (Figure 8). While we favor this as the most likely scenario, it is not possible at this point to rule out other less parsimonious alternatives. For example, perhaps NGA activates an unknown factor X, and this in turn heterodimerizes with HEC or vice versa, and putative X-HEC (or X-NGA) complexes are the functionally active heterodimers required for ultimately regulating *IND/SPT*. However, the proposed model is highly consistent with the results reported here and with other more indirect evidence. For example, whereas no ChIP-seq data are currently available for NGA transcription factors, several NGA binding motifs can be found in the promoters

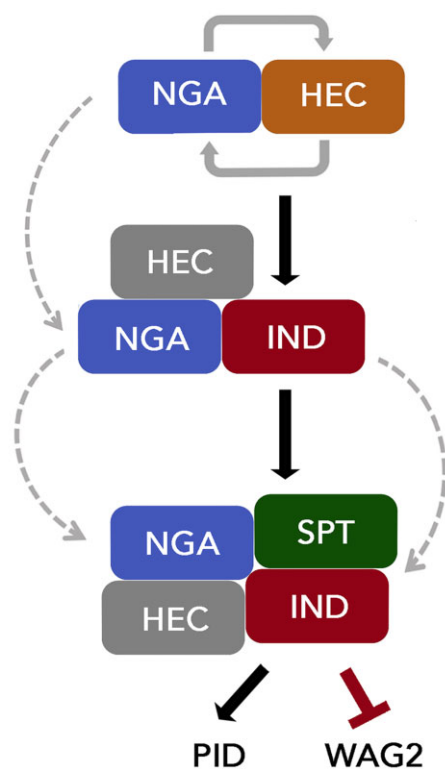


Figure 8 Proposed model for the sequential activation of transcription factors required for stigma development. HEC and NGA transcription factors are expressed in overlapping domains in the apical gynoecium of *Arabidopsis* prior to stigma differentiation, where they interact as a complex, likely reinforcing each other's expression (indicated by solid gray lines). This complex activates the expression of IND in this domain (indicated by a solid black arrow). Then, IND, NGA, and probably HEC (which now appears shadowed in gray because its incorporation into this complex is not fully validated and probably not essential) form a higher-order complex to activate SPT (indicated by a solid black arrow). SPT is subsequently incorporated into the IND–NGA–(HEC) complex to regulate other downstream targets such as PID or WAG2. Curved gray dashed lines represent the sequential incorporation of the different transcription factors into subsequent protein complexes.

of *IND*, *SPT*, *PID*, and *WAG2* genes. Together with the reported ability of NGA transcription factors to heterodimerize with IND and with SPT, this evidence supports the notion that IND and SPT associate with NGA (and likely also with HEC transcription factors) to form a multimeric complex that ultimately directs stigma specification.

The strict requirement for the presence of HEC in order to observe the whole spectrum of p35S:NGA3 visible phenotypes is in accordance with our model, but partly contradicts a previously reported study (Gaillochet et al., 2018). In this work, Gaillochet et al. show that (1) *NGA1* expression driven by the *CLAVATA3* (*CLV3*) promoter causes changes in stem cell regulation in the SAM that are similar in wild-type and *hec1 hec2 hec3* backgrounds, (2) conversely, the effect of *HEC1* misexpression in the SAM is not modified by the *nga1 nga2* mutations, and (3) simultaneous expression of *NGA1* and *HEC1* directed by this same *CLV3* promoter does not cause

major synergistic phenotypes. This apparent paradox can be explained based on differences between the two studies. In contrast to the strong localized expression provided by the *CLV3* promoter, the p35S:NGA3 transgene only provides moderate overexpression of NGA3. Moreover, in the present study, we only used hemizygote lines, since homozygous lines for the transgene are not fertile and tend to silence the transgene (Trigueros et al., 2009). Thus, if as we propose, NGA transcription factors form parts of functional transcriptional complexes, protein levels could be critical for determining the composition and activity of these complexes, and the strong accumulation of NGA transcription factors in the *CLV3* expression domain could promote alternative interactions or disrupt existing ones. In addition, despite the high level of redundancy found in the NGA subfamily, it is likely that the NGA1/NGA2 transcription factors have slightly different activities from NGA3/NGA4, including their interactions with HEC1/2 and HEC3. The finding that NGA3 has a stronger requirement for HEC3 in order to cause overexpression phenotypes provides support to this hypothesis.

It is also important to consider the likely participation of NGA transcription factors in alternative genetic pathways and/or transcriptional complexes with different activities and functions. Following a similar genetic approach, we previously showed that NGA and SHI/STY require each other (and likely additional factors) in order to promote style formation in specific domains of the ovary, suggesting that NGA and SHI/STY could cooperatively direct style morphogenesis together with yet unidentified genes (Trigueros et al., 2009). Interestingly, many genes involved in hormone signaling pathways have been identified as common transcriptional targets of the basic set of transcription factors directing style and stigma development, supporting the idea of their cooperative and combinatorial activity (Sorefan et al., 2009; Eklund et al., 2010; Sidaway-Lee et al., 2010; Josse et al., 2011; Reymond et al., 2012; Baylis et al., 2013; Martinez-Fernandez et al., 2014; Moubayidin and Ostergaard, 2014; Schuster et al., 2014; Gaillochet et al., 2017; Reyes-Olalde et al., 2017; Simonini et al., 2018). Finally, several studies report different feed-forward loops of cross-regulation among the factors involved in apical gynoecium development, which should be important for refining their spatiotemporal distribution (Alvarez et al., 2009; Girin et al., 2011; Staldal et al., 2012; Gaillochet et al., 2018). Altogether, this evidence supports the notion that a highly dynamic set of regulatory interactions occurs among the transcription factors directing apical gynoecium development. These interactions are likely mediated by the fine-tuned regulation of their expression levels and therefore their availability to participate in different transcriptional complexes, depending on the spatial and temporal context. Nevertheless, further studies are needed to confirm this hypothesis and unravel the molecular details.

Materials and methods

Plant material and growth conditions

Arabidopsis thaliana plants were grown in cabinets at 21°C under long day (16-h light) or short day (8-h light)

conditions, illuminated by cool-white fluorescent lamps ($150 \mu\text{mol m}^{-2} \text{s}^{-1}$), in a 1:1:1 mixture of sphagnum:perlite:vermiculite. To promote germination, seeds were stratified on soil at 4°C for 3 days in the dark.

Previously described *A. thaliana* lines used in this study included the following: *nga1*, *nga2*, *nga3*, *nga4*, *p35S:NGA3*, *pNGA3:GUS* (Trigueros et al., 2009), *hec1*, *hec3*, *hec1 hec3*, *pHEC1:HEC1:GUS*, *pHEC2:GUS*, *pHEC3:GUS* (Gremski et al., 2007), *ind1-2* (Liljegren et al., 2004), *spt-2* (Alvarez and Smyth, 1999), *ind-2 spt-12* (Girin et al., 2011), and *p35S:IND:GR*, *pIND:IND:GUS* (Sorefan et al., 2009).

The different genetic combinations were cross-fertilized, and all the combinations were identified among the F2 segregants based on novel phenotypes and confirmed by genotyping or by segregation of F3 progenies. Genotyping of *nga*, *hec*, *ind1-2*, and *spt-2* mutants was performed as previously described in Trigueros et al. (2009), Gremski et al. (2007), Liljegren et al. (2004), and Alvarez and Smyth (1999), respectively (Supplemental Table S1).

The *Arabidopsis* plants used in this work were in the Columbia-0 (Col-0) background, except for *spt-2*, which is in the Landsberg *erecta* ecotype (*Ler*) background.

Plasmid construction and *Arabidopsis* transformation

To generate the overexpression lines, the coding sequences of *HEC1* and *HEC3* were PCR amplified using Col genomic DNA as a template and the oPBF3–oPBF4 primers for *HEC1* and the oPBF7–oPBF8 primers for *HEC3* (Supplemental Table S1). The PCR product was cloned into the pCR8-GW-TOPO vector (Invitrogen) and *p35S:HEC1* and *p35S:HEC3* were generated by cloning the two different coding sequences into the pEarley100 vector via Gateway LR Clonase II recombination reaction (Earley et al., 2006). In both cases, the integrity of all constructs was confirmed by sequencing.

Finally, *Agrobacterium* strain C58 pM090 was used to transform *A. thaliana* wild-type and mutant plants using the floral dip method (Clough and Bent, 1998), and phenotypes were analyzed in the T1 and T2 generations.

GUS histochemical detection

For β -glucuronidase (GUS) histochemical detection, samples were treated for 15 min in 90% ice-cold acetone, washed for 5 min with washing buffer (25-mM sodium phosphate, 2-mM ferrocyanide, 2-mM ferricyanide, and 1% Triton X-100), and incubated from 4 to 16 h at 37°C in staining buffer (washing buffer + 1-mM X-glucuronide). Following staining, the plant material was fixed, cleared in chloral hydrate, and mounted according to Weigel and Glazebrook (2002) to be viewed under bright-field microscopy (Nikon Eclipse E-600). All detections were made in heterozygous lines for the reporter transgene.

Scanning electron microscopy

Flowers at anthesis and fruits for each genotype were fixed overnight at 4°C in FAE solution (ethanol:acetic acid:formaldehyde:water, 50:5:3.5:41.5, v/v/v/v), dehydrated through an

ethanol series, and critical-point dried in liquid CO_2 . The samples were coated with gold-palladium (4:1) and observed under a JEOL (JSM-5410) electronic microscope, working at 10–15 kV and a scanning speed of 200 s per image.

Bimolecular fluorescence complementation assay

The open reading frames of full-length *NGA1*, *NGA3*, *HEC1*, *HEC3*, *IND*, and *SPT* were PCR amplified using Col genomic DNA as a template and the following primer pairs, respectively: otl2THF–otl2THR, oMT1–oMT2, oPBF3–oPBF4, oPBF7–oPBF8, indATG F–indSTOP R, and SPT ATG–oPBF132 (Supplemental Table S1). The PCR products were cloned into the pCR8-GW-TOPO vector, and the different coding sequences were cloned into pYFPN43 and pYFPC43 vectors by Gateway LR Clonase II recombination reaction (Earley et al., 2006; Belda-Palazon et al., 2012). The BiFC assay was performed as previously described (Scacchi et al., 2009). The samples were observed by confocal microscopy (Leica TCS SL). Negative controls for interactions of *HEC1*, *HEC3*, *IND*, and *SPT* with *PISTILLATA* (*PI*), *NGA1* and *NGA3* with *FRUITFULL* (*FUL*), and *NGA1*, *NGA3*, *HEC1*, *HEC3* with *AKIN β 2* are shown in Supplemental Figure S2. The additional constructs for these controls are described in Balanzá et al. (2014) and Belda-Palazón et al. (2012).

Co-IP

The full-length coding sequences of *NGA3*, *HEC1*, *HEC3*, *IND*, and *SPT* were cloned into the pCR8-GW-TOPO (Invitrogen) vector and introduced into the pEarleyGate104, pEarleyGate202 and pEarleyGate203 vectors via Gateway LR Clonase II recombination reaction (Earley et al., 2006). Co-IP assays were performed in *N. benthamiana* leaves as described previously (Barja et al., 2021). The protein was extracted in lysis buffer (50-mM Tris–HCl, pH 7.5, 150-mM NaCl, 5% [v/v] glycerol, 0.1% [v/v] Triton, 1-mM MgCl_2 , 0.5-mM phenylmethylsulfonyl fluoride (PMSF), 10-mM DTT, 2% polyvinylpyrrolidone, $1\times$ cocktail protease inhibitor). CoIP samples were incubated with anti-GFP antibody (Invitrogen; A11122) overnight at 4°C , and immunoprecipitation was performed with Pierce Protein A/G Magnetic Beads (Thermo Scientific; 88802). The beads were washed three times with wash buffer (50-mM Tris–HCl, pH 7.5, 500-mM NaCl, 5% [v/v] glycerol, 0.1% [v/v] Triton, 1-mM MgCl_2 , 0.5-mM PMSF, 10-mM DTT, $1\times$ cocktail protease inhibitor). Finally, 1xGFP, 1xFlag, or 1xMyc fusion proteins were detected by immunoblotting with anti-GFP, anti-Flag (Sigma; A8592), or anti-c-Myc (Sigma; M4439) antibodies. A Supersignal West Femto Maximum Sensitive Substrate Detection Kit (Thermo Scientific; 34095) was used for detection, and the signal was visualized using the ImageQuant800 System (Amersham). Similar results were obtained from three biological repeats of the experiments, where each replicate consisted of pooled infiltrated leaves from different plants infiltrated and collected on the same or different days.

qRT-PCR expression analysis

The plant material used for qRT-PCR was inflorescences of the wild-type, *p35S:NGA3*, and the *nga* quadruple mutant and the primers used were qHEC1F and qHEC1R for *HEC1*, qHEC2F, and qHEC2R for *HEC2*, and qHEC3F and qHEC3R for *HEC3*; 10-day-old wild-type, *p35:NGA3* and *p35S:NGA3* *hec1 hec3* seedlings with primers NGA3-F and NGA3-R for *NGA3*. Seeds from *A. thaliana p35S:IND:GR* and *p35S:IND:GR nga1 nga3 nga4* were germinated in 0.5 × Murashige and Skoog medium with constant shaking. We then treated 7-day-old seedlings for 4 h with 10-μM Dex or Mock. Primers used were as follows: WAG2-F and WAG2-R for *WAG2*, PID-F and PID-R for *PID*, and oSPT F_qPCR and oSPT R_qPCR for *SPT* (Supplemental Table S1).

Results were normalized to the expression of *TIP41-LIKE* (*TIP41*) amplified with qRT-TIP41F and qRT-TIP41R primers, or *UBIQUITIN* (*UBQ*) amplified with qUBQ F and qUBQ R primers (Supplemental Table S1).

Total RNA was extracted from the samples with an E.Z.N.A. Plant RNA Kit (OMEGA Bio-Tek, Doraville, GA, USA). Three micrograms of total RNA were used for cDNA synthesis with a First Strand cDNA Synthesis Kit (Invitrogen, Carlsbad, CA, USA), and quantitative PCR master mix was prepared using SYBR Premix Ex Taq (Takara Co., Tokyo, Japan). The PCR reactions were run and analyzed using the 7500 Fast Real-Time PCR System (Applied Biosystems, Foster City, CA, USA). The program was as follows: 50°C for 2 min, melting at 95°C for 10 min, and amplification with 40 cycles of 95°C for 15 s, followed by 60°C for 1 min. The analyses were performed in three biological replicates of pooled samples from three to five different plants grown simultaneously, each with three technical replicates. The Student's *t* test was used to determine the significance of expression level differences.

ChIP

p35S:IND:GR and *p35S:IND:GR nga1 nga3 nga4* plants were grown for 6 weeks, after which all inflorescence meristems were treated with 20 μM of Dex or Mock solution. Approximately 0.7 g of tissue was harvested per sample. Immunoprecipitation with GR antibody (ABCAM, ab3580) was performed as previously described in Sorefan et al. (2009) and Girin et al. (2011). The analyses were performed in three biological replicates of pooled samples from 10 to 15 different plants grown and treated simultaneously.

Statistical analysis

The figures show the sample mean ± SD. Pairwise comparisons between the means of different samples were performed using a two-sided Student's *t* test, using Microsoft Excel 2016 software.

Accession numbers

Sequence data from this article can be found in the Arabidopsis Genome Initiative or GenBank/EMBL databases under the following accession numbers: NGA1(AT2G46870), NGA2 (AT3G61970), NGA3 (AT1G01030), NGA4

(AT4G01500), HEC1 (AT5G67060), HEC2 (AT3G50330), HEC3 (AT5G09750), IND (AT4G00120), SPT (AT4G36930), PID (AT2G34650), WAG2 (AT3G14370), TIP-41(AT4G34270), UBQ (AT4g36800), PI (At5g20240), FUL (AT5G60910), AKINβ2 (At4g16360).

Supplemental data

The following materials are available in the online version of this article.

Supplemental Figure S1. Phenotypes of plants with different combinations of *p35S:NGA3* and *hec1* and *hec3* mutations.

Supplemental Figure S2. BiFC negative controls.

Supplemental Table S1. Primers used in this study.

Acknowledgments

We thank Lars Ostergaard (JIC, UK) and Martin F. Yanofsky (UCSD, USA) for sharing material and Miguel Blázquez and Francisco Madueño (IBMCP) for helpful discussion. We also thank Carolina del Cerro and Maria Jose Domenech for excellent technical assistance, members of David Alabadí lab (IBMCP) for technical advice and Marisol Gascón (IBMCP) for technical advice with confocal and DIC microscopy.

Funding

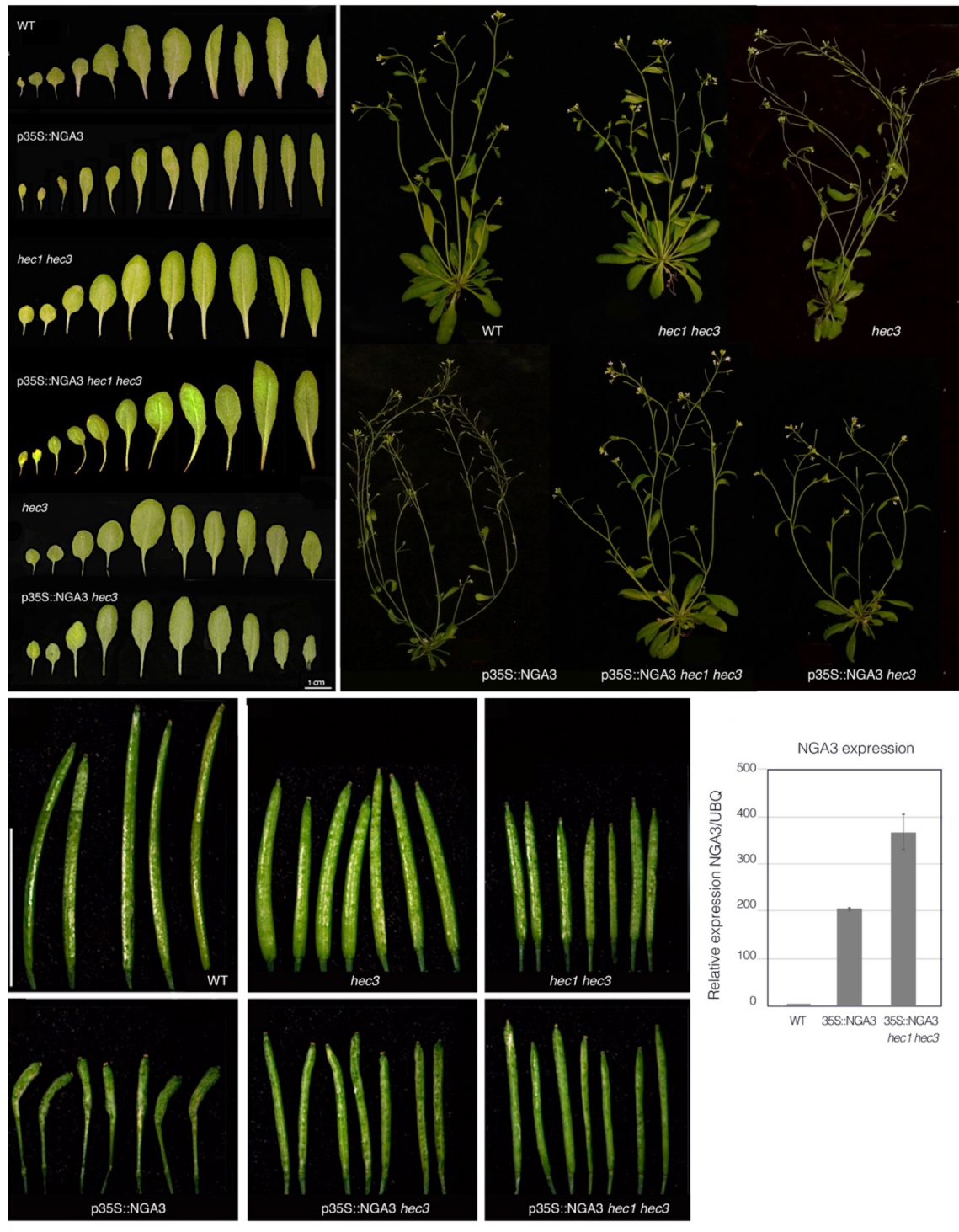
This work was supported by the Spanish Ministerio de Economía y Competitividad (grant BIO2015-64531-R to C.F.) and the Spanish Ministerio de Ciencia, Innovación y Universidades (grant RTI2018-099239-B-I00 to C.F.).

Conflict of interest statement. None declared.

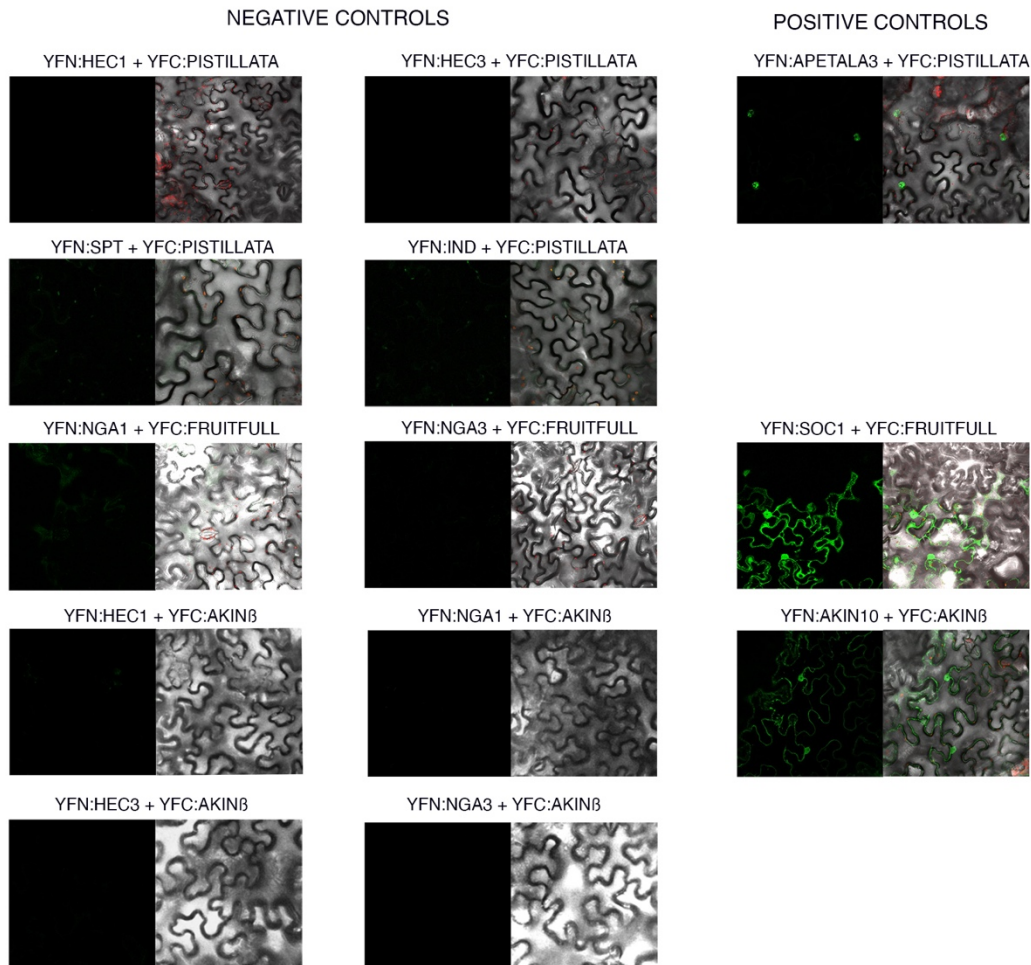
References

- Alvarez J, Smyth DR (1999) CRABS CLAW and SPATULA, two Arabidopsis genes that control carpel development in parallel with AGAMOUS. *Development* **126**: 2377–2386
- Alvarez JP, Goldshmidt A, Efroni I, Bowman JL, Eshed Y (2009) The NGATHA distal organ development genes are essential for style specification in Arabidopsis. *Plant Cell* **21**: 1373–1393
- Alvarez JP, Furumizu C, Efroni I, Eshed Y, Bowman JL (2016) Active suppression of a leaf meristem orchestrates determinate leaf growth. *eLife* **5**
- Balanà V, Martínez-Fernández I, Ferrándiz C (2014) Sequential action of FRUITFULL as a modulator of the activity of the floral regulators SVP and SOC1. *J Exp Bot* **65**: 1193–1203
- Ballester P, Navarrete-Gomez M, Carbonero P, Onate-Sanchez L, Ferrándiz C (2015) Leaf expansion in Arabidopsis is controlled by a TCP-NGA regulatory module likely conserved in distantly related species. *Physiol Plant* **155**: 21–32
- Barja MV, Ezquerro M, Beretta S, Diretto G, Florez-Sarasa I, Feixes E, Fiore A, Karlova R, Fernie AR, Beekwilder J, et al. (2021) Several geranylgeranyl diphosphate synthase isoforms supply metabolic substrates for carotenoid biosynthesis in tomato. *New Phytol* **231**: 255–272
- Baylis T, Cierlik I, Sundberg E, Mattsson J (2013) SHORT INTERNODES/STYLISH genes, regulators of auxin biosynthesis, are involved in leaf vein development in Arabidopsis thaliana. *New Phytol* **197**: 737–750
- Belda-Palazón B, Ruiz L, Martí E, Tárraga S, Tiburcio AF, Culiáñez F, Farràs R, Carrasco P, Ferrando A (2012)

- Aminopropyltransferases involved in polyamine biosynthesis localize preferentially in the nucleus of plant cells. *PLoS one* 7: e46907
- Clough SJ, Bent AF** (1998) Floral dip: a simplified method for *Agrobacterium*-mediated transformation of *Arabidopsis thaliana*. *Plant J* 16: 735–743
- Earley KW, Haag JR, Pontes O, Opper K, Juehne T, Song K, Pikaard CS** (2006) Gateway-compatible vectors for plant functional genomics and proteomics. *Plant J* 45: 616–629
- Eklund DM, Staldal V, Valsecchi I, Cierlik I, Eriksson C, Hiratsu K, Ohme-Takagi M, Sundstrom JF, Thelander M, Ezcurra I, et al.** (2010) The *Arabidopsis thaliana* STYLISH1 protein acts as a transcriptional activator regulating auxin biosynthesis. *Plant Cell* 22: 349–363
- Ferrandiz C, Fourquin C, Prunet N, Scutt C, Sundberg E, Trehin C, Viale-Guiraud A** (2010) Carpel development. *Adv Bot Res* 55: 1–74
- Fourquin C, Ferrandiz C** (2014) The essential role of NGATHA genes in style and stigma specification is widely conserved across eudicots. *New Phytol* 202
- Gaillochet C, Jamge S, van der Wal F, Angenent G, Immink R, Lohmann JU** (2018) A molecular network for functional versatility of HECATE transcription factors. *Plant J* 95: 57–70
- Gaillochet C, Stiehl T, Wenzl C, Ripoll JJ, Bailey-Steinitz LJ, Li L, Pfeiffer A, Miotk A, Hakenjos JP, Forner J, et al.** (2017) Control of plant cell fate transitions by transcriptional and hormonal signals. *eLife* 6
- Girin T, Paicu T, Stephenson P, Fuentes S, Körner E, O'Brien M, Sorefan K, Wood TA, Balanzá V, Ferrándiz C, et al.** (2011) INDEHISCENT and SPATULA interact to specify carpel and valve margin tissue and thus promote seed dispersal in *Arabidopsis*. *Plant Cell* 23: 3641–3653
- Gomariz-Fernandez A, Sanchez-Gerschon V, Fourquin C, Ferrandiz C** (2017) The role of SHI/STY/SRS genes in organ growth and carpel development is conserved in the distant eudicot species *Arabidopsis thaliana* and *Nicotiana benthamiana*. *Front Plant Sci* 8: 814
- Gremski K, Ditta G, Yanofsky MF** (2007) The HECATE genes regulate female reproductive tract development in *Arabidopsis thaliana*. *Development* 134: 3593–3601
- Heisler M, Atkinson A, Bylstra Y, Walsh R, Smyth D** (2001) SPATULA, a gene that controls development of carpel margin tissues in *Arabidopsis*, encodes a bHLH protein. *Development* 128: 1089–1098
- Ichihashi Y, Horiguchi G, Gleissberg S, Tsukaya H** (2010) The bHLH transcription factor SPATULA controls final leaf size in *Arabidopsis thaliana*. *Plant Cell Physiol* 51: 252–261
- Josse EM, Gan Y, Bou-Torrent J, Stewart KL, Gilday AD, Jeffrey CE, Vaistij FE, Martinez-Garcia JF, Nagy F, Graham IA, et al.** (2011) A DELLA in disguise: SPATULA restrains the growth of the developing *Arabidopsis* seedling. *Plant Cell* 23: 1337–1351
- Kuusk S, Sohlberg JJ, Magnus Eklund D, Sundberg E** (2006) Functionally redundant SHI family genes regulate *Arabidopsis* gynoecium development in a dose-dependent manner. *Plant J* 47: 99–111
- Liljegren SJ, Roeder AHK, Kempin SA, Gremski K, Østergaard L, Guimil S, Reyes DK, Yanofsky MF** (2004) Control of fruit patterning in *Arabidopsis* by INDEHISCENT. *Cell* 116: 843–853
- Martinez-Fernandez I, Sanchis S, Marini N, Balanza V, Ballester P, Navarrete-Gomez M, Oliveira AC, Colombo L, Ferrandiz C** (2014) The effect of NGATHA altered activity on auxin signaling pathways within the *Arabidopsis* gynoecium. *Front Plant Sci* 5: 210
- Moubayidin L, Ostergaard L** (2014) Dynamic control of auxin distribution imposes a bilateral-to-radial symmetry switch during gynoecium development. *Curr Biol* 24: 2743–2748
- Reyes-Olalde JI, Zuniga-Mayo VM, Serwatowska J, Chavez Montes RA, Lozano-Sotomayor P, Herrera-Ubaldo H, Gonzalez-Aguilera KL, Ballester P, Ripoll JJ, Ezquer I, et al.** (2017) The bHLH transcription factor SPATULA enables cytokinin signaling, and both activate auxin biosynthesis and transport genes at the medial domain of the gynoecium. *PLoS Genet* 13: e1006726
- Reymond MC, Brunoud G, Chauvet A, Martinez-Garcia JF, Martin-Magniette ML, Moneger F, Scutt CP** (2012) A light-regulated genetic module was recruited to carpel development in *Arabidopsis* following a structural change to SPATULA. *Plant Cell* 24: 2812–2825
- Scacchi E, Osmont KS, Beuchat J, Salinas P, Navarrete-Gómez M, Trigueros M, Ferrándiz C, Hardtke CS** (2009) Dynamic, auxin-responsive plasma membrane-to-nucleus movement of *Arabidopsis* BRX. *Development* 136: 2059–2067
- Schuster C, Gaillochet C, Lohmann JU** (2015) *Arabidopsis* HECATE genes function in phytohormone control during gynoecium development. *Development* 142: 3343–3350
- Schuster C, Gaillochet C, Medzihradsky A, Busch W, Daum G, Krebs M, Kehle A, Lohmann JU** (2014) A regulatory framework for shoot stem cell control integrating metabolic, transcriptional, and phytohormone signals. *Dev Cell* 28: 438–449
- Sidaway-Lee K, Josse EM, Brown A, Gan Y, Halliday KJ, Graham IA, Penfield S** (2010) SPATULA links daytime temperature and plant growth rate. *Curr Biol* 20: 1493–1497
- Simonini S, Stephenson P, Ostergaard L** (2018) A molecular framework controlling style morphology in Brassicaceae. *Development* 145
- Sorefan K, Girin T, Liljegren SJ, Ljung K, Robles P, Galván-Ampudia CS, Offringa R, Friml J, Yanofsky MF, Ostergaard L** (2009) A regulated auxin minimum is required for seed dispersal in *Arabidopsis*. *Nature* 459: 583–586
- Staldal V, Cierlik I, Chen S, Landberg K, Baylis T, Myrenas M, Sundstrom JF, Eklund DM, Ljung K, Sundberg E** (2012) The *Arabidopsis thaliana* transcriptional activator STYLISH1 regulates genes affecting stamen development, cell expansion and timing of flowering. *Plant Mol Biol* 78: 545–559
- Trigueros M, Navarrete-Gómez M, Sato S, Christensen SK, Pelaz S, Weigel D, Yanofsky MF, Ferrándiz C** (2009) The NGATHA genes direct style development in the *Arabidopsis* gynoecium. *Plant Cell* 21: 1394–1409
- Weigel D, Glazebrook J** (2002) Cold Spring Harbor Laboratory Press, Cold Spring Harbor, New York



Supplemental Figure S1. Phenotypes of plants with different combinations of p35S:NGA3 and *hec1* and *hec3* mutations. Supports Figure 1. Top left: The leaves of individual plants with the indicated genotypes are shown. Top right: individual plants with the indicated genotypes are shown. While the rosette of p35S:NGA3 is reduced in size and shows narrow leaves, *hec* mutations partially (*hec3*) or completely (*hec1 hec3*) suppress these defects. Bottom left: fully elongated fruits of the indicated genotypes. *hec3* and *hec1 hec3* fruits have similar shape to those of Columbia wild type, only shorter, while 35S:NGA3 fruits show strong alterations in development. *hec* mutations partially (*hec3*) or completely (*hec1 hec3*) suppress these defects. Bottom right: Quantification of *NGA3* expression level by qRT-PCR in WT (Col), 35S:NGA3 and 35S:NGA3 *hec1 hec3* lines showing that the 35S:NGA3 also drives high levels of *NGA3* expression in the *hec1 hec3* background. Error bars indicate standard deviation of the mean of three biological replicates.



Supplemental Figure S2. BiFC negative controls. Supports Figures 3 and 7. The YFN:HEC1/HEC3/IND/SPT constructs were co-infiltrated with a vector containing a YFC:PISTILLATA coding sequence. The YFN:NGA1/NGA3 constructs were co-infiltrated with a vector containing a YFC:FRUITFULL coding sequence. PISTILLATA and FRUITFULL are unrelated MADS-box transcription factors. In all cases, no reconstituted fluorescence was observed.

YFN:HEC1/HEC3/NGA1/NGA3 constructs were also co-infiltrated with YFC:AKIN β 2, a subunit of the Arabidopsis SnRK kinase that localizes to both the cytoplasm and the nucleus.

Positive controls for well-known interactions of the MADS box factors PISTILLATA with APETALA3 and SOC1 with FRUITFULL, and of two subunits of the SnRK kinase complex, AKIN10 with AKIN β 2, are also provided.

Supplemental Data. Ballester et al. (2021). A transcriptional complex of NGATHA and bHLH transcription factors directs stigma development in Arabidopsis. Plant Cell.

Primer	Sequence	Purpose
oTOL2Rwt SS071 P745 oMNG15 oMNG14 EN8130 SS43 SS44 SS65 SS66	5_-AGCAGCAGCAGCAGCCATATTTAG-3_ 5_-AACGTCATCATCACAGTGGTGGTGG-3_ 5_-AACGTCCGCAATGTGTTATTAAGTTGTC-3 5_-CCAACCATAGAACTCTGCC-3_ 5_-CGACAAAGTAGTAACACCAAG-3_ 5_-GAGCGTCGGTCCCCACACTTCTATAC-3 5_-CCAACGGCTCTGATCCAACAATG-3 5_-ACCGTCGACAATAACATATACATAC-3 5_-CCTCTCGAGTGATACTTTTGTGAATATCTCAAC-3_ 5_-GGAGGATCCTCTTCAAAGCTCTAAAGATTTCCC-3_	<i>nga</i> mutants genotyping
oKG156 oKG157 Gabi-T	5_-ACCACAACAACACTTACCCTTTTC-3 5_-GTTCCACACCCTTTTATAACCACT-3_ 5_-CCCATTTGGACGTGAATGTAGACAC-3	<i>hec1</i> genotyping
ILC-X8 ILC-X3 LBb3	5_-GTGCTATTTTCGTGAAGAGACAAGAGA-3 5_-TCCTAACAACCCTTATTTTCGTATCCA-3 5_-ACCCAGCGTGGACCGCTTGGTG-3	<i>hec3</i> genotyping
oMT15 oMT16	5_-GTTTATCTTTCTTGTCCCAGAGGA-3 5_-ATCAAGCATTGAAGCCTTATCCGT-3	<i>spt-2</i> genotyping
GT140-P GT140-Q	5_-GCTAATGATCTTCTCACACAAGAAC-3_ 5_-ATCGCATCCATGTCTTCATCGTAC-3	<i>ind1-2</i> genotyping
qNGA3 F qNGA3 R qHEC1 F qHEC1 R qHEC2 F qHEC2 R qHEC3 F qHEC3 R WAG2-F WAG2-R PID-F PID-R oSPT F_qPCR oSPT R_qPCR qUBQ F qUBQ R qRT-TIP41 F qRT-TIP41 R	5_-GAGGTATTTCCCTCTAGACTC-3 5_-GAGACAATGTCTCCTGCATC-3 5_-GGGGGAGTGGTTATGAAAGGGTGT-3_ 5_-TGCATTGCCACCATCTGATGAGT-3_ 5_-TGCGGGTACTGTTGGTGGAGGATA-3 5_-TGATCAGACCGCATAATGCCACAC-3_ 5_-ACCTGGCACGAGTCTCTGAAGAA-3 5_-GGCTAGACATCGCCGTGAGAGAAT-3 5_-GACGGACACGTCATGTTGTCCGA-3 5_-GTGTCCGTTGCCGAAACTAGCT-3_ 5_-GCCAGATTTTATGCCGCCGAAGT-3 5_-GAAGACGAGGAAGATTCAACGGCT-3 5_-GAAGGACCTGACTTGGAGAGGGGA-3 5_-TGTGAAAGCGAGGAAGGAGGAGAA-3 5_-CTGTTACGGAACCCAATTC-3 5_-GGAAAAAGGTCTGACCGACA-3 5_-GTGAAAACCTGTTGGAGAGAAGCAA-3_ 5_-TCAACTGGATACCCTTTTCGCA-3	qRT-PCR
oPBF3 oPBF4	5_-ATGAATAATTATAATATGAACCCAT-3 5_-CTAGATTAATTCTCCTACTCCTCT-3	<i>HEC1</i> CDS cloning
oPBF7 oPBF8	5_-ATGGATTCTGACATAATGAACATGA-3_ 5_-TCATCTAAGAATCTGTGCATTGC-3	<i>HEC3</i> CDS cloning
otl2THF otl2THR	5_-GAATCCATGATGACAGATTTA-3_ 5_-GTCGACTTGATCCAAATCAAA-3	<i>NGA1</i> CDS cloning
OMT1 OMT2	5_-GGATCCATGGATCTATCCCTGG-3 5_-GAGCTCTGGATTGAAATTGAGAGA-3_	<i>NGA3</i> CDS cloning
ind ATG F ind STOP R	5_-ATGGAAAATGGTATGTATAAA-3 5_-TCAGGGTGGGAGTTGTGGTA-3	<i>IND</i> CDS cloning
SPT ATG oPBF132	5_-ATGATATCACAGAGAGAAGAAAG-3_ 5_-TCAAGTAATTCGATCTTTTAGG-3	<i>SPT</i> CDS cloning
WAG2F WAG2R PID-678F PID-368R SPT473 SPT776 Mu-like-F Mu-like-R ACT f ACT R NRT2.1-F NRT2.1-R	5_-CCGACCGTACATTCACCTCATCAAG-3_ 5_-ATCCGGTAGGGTTAGGGCAATCA-3 5_-TTCGTTTATTCTAGCCATTTTACA-3 5_-CCTCTCGCTAATTTTTGTTTTGTT-3 5_-GATCCCTGTTTAATTTGACGATT-3 5_-TGCAACATTCACTTAACCTCGTAT-3_ 5_-GATTTACAAGGAATCTGTTGGTGGT-3 5_-CATAACATAGGTTTAGAGCATCTGC-3 5_-CGTTTCGCTTTCCCTTAGTGTTAGCT-3 5_-AGCGAACGGATCTAGAGACTCACCTTG-3 5_-AACAAAGGGCTAACGTGGATG-3_ 5_-CTGCTTCTCCTGCTCATTCC-3	ChIP

Supplemental Table S1. Primers used in this study.